

coplanar with the cyano groups to which they are bonded.

The structure model described above holds also for $K_2[Pt(CN)_4]Br_{0.3} \cdot 3H_2O$ and for the original intensity data published by Krogmann and Hausen⁵ as R values for the superstructure reflections of 0.11 show.

We hope to obtain more precise results especially concerning the Pt arrangement from low-temperature investigations which are now in progress.

We are indebted to K. Krogmann for informative discussions. Furthermore we thank H. Heyzenau for stimulating this work, and H. J. Queisser and A. Rabenau for critical reading.

¹For a recent review see H. R. Zeller, in *Festkör-*

perprobleme, edited by H. J. Queisser (Vieweg, Braunschweig, 1973), Vol. XIII, p. 31.

²B. Renker, L. Pitschovius, W. Gläser, H. Rietschel, R. Comés, L. Liebert, and W. Drexel, *Phys. Rev. Lett.* **32**, 836 (1974).

³P. A. Lee, T. M. Rice, and P. W. Anderson, *Phys. Rev. Lett.* **31**, 462 (1973).

⁴R. Comés, M. Lambert, and H. Launois, *Phys. Rev. B* **8**, 571 (1973).

⁵K. Krogmann and H.-D. Hausen, *Z. Anorg. Allg. Chem.* **358**, 67 (1968).

⁶The work was done in close contact with K. Krogmann, who also supplied us with the crystals.

⁷ $\sigma(I)$ is the standard deviation calculated from the counting statistics of the net intensity I .

⁸Lattice constants $a = b = 9.866 \text{ \AA}$, $c = 5.773 \text{ \AA}$ (Ref. 5).

⁹G. H. Stout and L. H. Jensen, *X-Ray Structure Determination* (Macmillan, London, 1970), p. 270.

¹⁰Wyckoff notation of equipoints in *International Tables for X-Ray Crystallography* (Kynoch Press, Birmingham, England, 1969), Vol. I, p. 189.

Phonon Broadening of X-Ray Photoemission Linewidths

P. H. Citrin, P. Eisenberger, and D. R. Hamann

Bell Laboratories, Murray Hill, New Jersey 07974

(Received 15 July 1974)

The significant contribution of phonon broadening to x-ray photoemission linewidths in polar materials has been experimentally verified. A simple theoretical expression is shown to account for the observed magnitude, temperature dependence, and variation with chemical environment of the photoemission widths.

Among the first workers to appreciate and explain the important contribution of vibrational structure to measured linewidths were those in the field of optical absorption.¹ Phonon production was later postulated to exist in situations where the rapidly formed core hole state resulted in x-ray,² photoelectron,³ or Auger-electron⁴ production. In x-ray photoemission linewidth studies [x-ray photoemission spectroscopy (XPS) or electron spectroscopy for chemical analysis (ESCA)] of gases and solids in which strong chemical effects were observed,^{5,6} the interpretation of the results had been complicated by an inexact knowledge of core-hole-state lifetimes and, in insulators, by the magnitude of possible charging effects. In very recent XPS linewidth⁷ and low-kinetic-energy Auger-electron-spectroscopy (AES) studies, the lifetime contribution, charging effects, and other potential sources were evaluated and found to be much too small to explain the observed linewidths. In this Letter we show that the excess linewidth broadening arises from the

production of large numbers of phonons simultaneous with core-hole formation. This work represents the first experimental verification of the presence of phonon broadening in XPS of solids and, in addition, provides a semiquantitative theory which accurately predicts the magnitude of the phonon contribution and its temperature dependence. The appreciably large phonon contribution is seen to be important for *all* XPS (and AES) studies of polar materials and thus represents the limiting factor in experimental linewidth resolution and accurate hole-state lifetime determinations. Vibrational broadening is also important to XPS (and AES) studies of gases and an XPS study of such effects in several gases has been recently reported.⁹

Phonon production in an XPS core-electron measurement in an insulating material arises from the different relaxation times for nuclei and electrons (the Franck-Condon principle) and the inability of the passive electrons surrounding the photohole to screen it from the rest of the lat-

tice. There is thus always a finite probability of exciting an electron into the continuum and leaving the remaining lattice in a vibrationally excited state. The probability of being in a particular state depends on the overlap of initial- and final-state wave functions, appropriately described in terms of the initial nuclear fluctuations (zero-point motion and thermal population) and final nuclear displacements upon relaxation. The measured width therefore contains an envelope of various excited final states, the number and intensity of which depend on the overlap factors and the degree of relaxation.

We may calculate the magnitude of XPS phonon linewidths in solids using the basic postulates of Huang and Rhys.¹⁰ By use of the Born-Oppenheimer approximation applied to an Einstein lattice which responds harmonically to a hole with a longitudinal optical frequency ω_{LO} , and with the assumption that the nuclear relaxation energy $\Delta E \gg \hbar\omega_{LO}$ (i.e., sufficient energy is available to excite a large number of phonons so that the Franck-Condon envelope or line-shape function is Gaussian¹), the linewidth (full width at half-maximum) at temperature T can be expressed as

$$\Gamma = 2.35[\hbar\omega_{LO}\Delta E]^{1/2}[\coth(\hbar\omega_{LO}/2kT)]^{1/2}. \quad (1)$$

The assumptions of this approach have been shown to be excellent first approximations to the actual situation.¹ The nuclear relaxation energy ΔE is calculated from the standard electron-LO-phonon interaction Hamiltonian representing the final-state core hole as completely localized.¹¹ The result is

$$\Delta E = e^2(6/\pi V_m)^{1/3}(1/\epsilon_\infty - 1/\epsilon_0), \quad (2)$$

where ϵ_0 and ϵ_∞ are the low- and high-frequency dielectric constants, and V_m is the volume of a primitive unit cell. The result of substituting (2) in (1) is similar to a formula derived by Overhauser¹² from a different point of view (but one that is essentially equivalent within the harmonic approximation), namely, calculating the fluctuation amplitude of the potential felt by the core electron in its initial state. The only significant difference in the formulas is that ours is based on the empirical ϵ_0 , while his contains a theoretical estimate.

From Eqs. (1) and (2), knowledge of a compound's crystal structure and its phonon and dielectric properties allows one readily to calculate temperature-dependent linewidths which may be compared with experiment. A thermally stable class of simple polar compounds whose

properties have been well characterized is the alkali halides, so these were chosen for the present study. Very thin films of ultrapure alkali-halide samples were evaporated at room temperature onto polished Cu substrates in the sample chamber of a Hewlett-Packard 5950A ESCA spectrometer. Film thicknesses were estimated to be typically $< 50 \text{ \AA}$ based on empirical halide/substrate photoline intensity ratios. Using very thin films in these, as in previous,⁶ measurements ensures minimal charge accumulation.¹³ Aside from improved resolution due to the essential absence of such charging, spectral detail of measured valence bands and energy-loss peaks were in excellent agreement with those observed in single-crystal XPS data.¹⁴ Oxygen and carbon contamination on the films was virtually nonexistent during the typical 12-h runs taken at nominal working pressures in the analyzer region of $\sim 2 \times 10^{-9}$ Torr. The linewidths of the most narrow (and/or intense) core lines for both cation and anion in a given compound were studied as a function of temperature up to the limiting Hewlett-Packard probe temperature of 550°K. The increased ionic mobility at higher temperatures aided in further reducing any residual sample charging.

Typical photoemission spectra of K $2p$ electrons in KI at three different temperatures are shown in Fig. 1. The data were fitted with a nonlinear least-squares fitting procedure using a linear background and line shape linearly adjustable between Gaussian and Lorentzian. In the absence of fitting constraints, spin-orbit intensity ratios from the fits agreed with statistical ratios to within 3%; standard deviations of the fitted linewidths were typically 0.01 eV. The line shapes of the fitted data were determined to be about 85% Gaussian.¹⁵

As examples of determining fractional phonon contributions to XPS linewidths we consider the K $2p_{3/2}$ electron lines measured in KF, KCl, and KI. These widths, determined from the above mentioned fits, are shown as filled circles and are plotted as a function of temperature in Fig. 2. Assuming XPS core line shapes to be Voigt functions (i.e., convoluted Lorentzian and Gaussian), a calculated atomic K $2p_{3/2}$ lifetime of 0.23 eV¹⁶ is used to determine the linewidth of the remaining total Gaussian component.¹⁷ Having obtained this Gaussian component, the essentially Gaussian instrumental contribution of 0.55 eV can then be easily removed. The resulting linewidths are shown as open circles in Fig. 2.

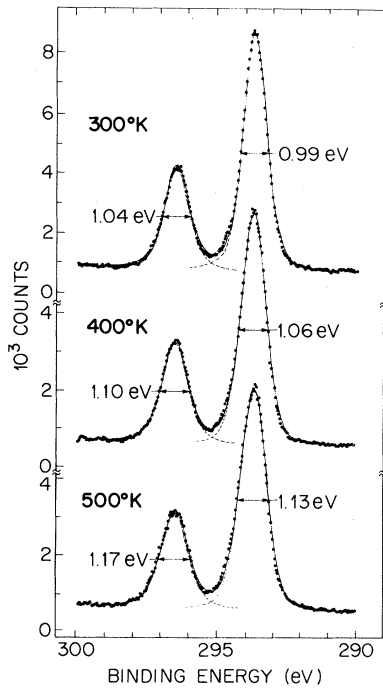


FIG. 1. X-ray photoemission spectra of K $2p_{3/2}$ and K $2p_{1/2}$ electrons in KI at 300, 400, and 500°K. Each channel is 0.039 eV.

The magnitude of these linewidths compares favorably with those calculated by using Eqs. (1) and (2) and the appropriate empirical constants; the results of such calculations are shown in Fig. 2 as solid lines. As already mentioned, the criterion for assuming Gaussian phonon broadening is that $\Delta E \gg \hbar\omega_{LO}$. In KI, for example, the coupling constant $S = \Delta E / \hbar\omega_{LO}$ is calculated to be as high as $(0.94 \text{ eV}) / (0.017 \text{ eV}) = 55$, well meeting this criterion for strong electron-phonon coupling. Thus, the only other Gaussian contribution so far unaccounted for is that arising from inhomogeneous sample charging. The effects and trends of such charging in these experiments are summarized and understood as follows: (1) For KF and KCl, the measured linewidths in the *negative*-sloped regions of the Γ -versus- T curves relative to those in the positive-sloped regions (see Fig. 2) correlate with observed higher apparent binding energies for both cations and anions; (2) the band gaps in these materials, which in large measure determine the magnitude of sample charging,¹³ decrease in the order KF > KCl > KI; (3) the ionic mobilities, which decrease the effects of charging, increase with T in the order KF < KCl < KI; and (4) the KF film was the thickest of the potassium halides

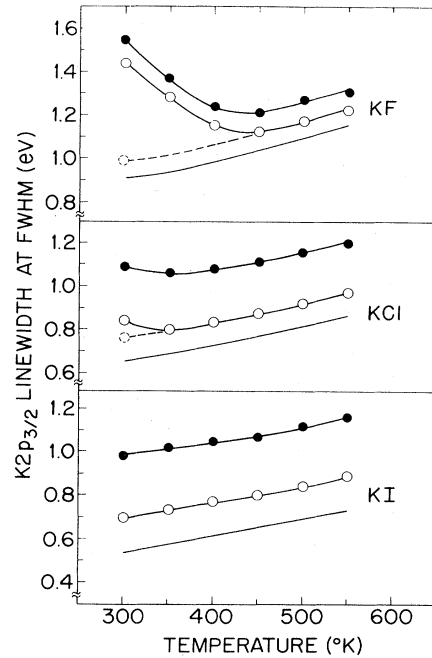


FIG. 2. K $2p_{3/2}$ linewidth (full width at half-maximum) versus temperature in KF, KCl, and KI. Filled circles are measured widths, open circles are the widths after removing lifetime and instrumental contributions, solid line is theoretical. Dashed extrapolated curve is hypothetical width in the absence of sample charging.

studied. We therefore interpret the agreement of the *positive*-sloped portion of the Γ -versus- T curves, where charging is minimal, as direct evidence for the effects of phonon broadening. This interpretation is supported not only by the agreement between trends of experimental and theoretical curves but also by the agreement of absolute magnitudes of the linewidth values and their temperature dependences: The calculated linewidths for KF, KCl, and KI are, respectively, about 95%, 90%, and 80% of the measured values at elevated temperatures, while the calculated total changes in linewidth from 300°K to 550°K all agree to within 0.03 eV of the measured changes if the experimental widths for KF and KCl are extrapolated to the limit of zero sample charging (shown as dashed curves in Fig. 2).

From consideration of Eqs. (1) and (2), these observations and comments readily follow: (1) Only for polar materials will phonon broadening be a dominant factor in XPS linewidth measurements because a sizable induced "nuclear dipole" must be formed, i.e., $1/\epsilon_\infty - 1/\epsilon_0$ in Eq. (2) must be large. (2) The temperature depen-

dences of the various potassium halides, for example, are very similar despite their significant lattice and dielectric properties because the *products* of the *two* terms in Eq. (1) are of comparable magnitude. (3) The Γ 's of anions have temperature dependences identical to those of cations in the same material and have magnitudes which are slightly smaller by ~ 0.1 – 0.2 eV. The reason for this is that, while to a first approximation the induced nuclear dipole is the same for the different ions, their nearest neighbors move (relax) far enough to feel nonlinear effects, and move in opposite directions in the two cases. (4) The chemical variation of XPS linewidths generally goes as $a^{-2}(\omega_{LO}\mu)^{-1/2}$, where a is the interatomic distance and μ is a reduced mass. This result can be seen from a simple model for the induced nuclear dipole energy: $\Delta E \propto \alpha_n e^2/a^4$; $\alpha_n = e^2/k_n = e^2/\mu\omega_{LO}^2$, where α_n and k_n are the nuclear polarizability and force constant, respectively. The trends predicted from this model have been observed in Na, Mg, and Al compounds⁶ and in mixed-valence materials such as NH_4NO_3 and $\text{Na}_2\text{S}_2\text{O}_3$.⁵

There are several important consequences and conclusions of this present work: (1) All XPS linewidths measured from polar materials will contain an appreciable contribution of phonon broadening. As a result, for these materials the XPS technique is inherently limited in ultimate resolution and ability to obtain accurate hole-state lifetime values. (2) The above conclusions apply also to gases,⁹ but for these species the magnitude of the broadening will also depend in large measure on the number of atoms (i.e., the number of possible vibrational modes) in the molecule. Thus, the C 1s linewidth in CH_4 , which has a coupling constant S of only 3,¹⁸ has been measured to be asymmetric^{9,19} (as is a Poisson distribution of very few events²⁰) whereas the C 1s linewidths for any of the C atoms in $\text{CF}_3\text{CO}_2\text{C}_2\text{H}_5$ are quite broad and symmetric.¹⁹ By analogy to the above mentioned solid-state considerations, we believe that the chemical dependence of gas-phase XPS linewidths⁵ can also be explained by phonon broadening. For example, the narrower N 1s width of the central N atom relative to the end N atom in linear $\text{N}=\text{N}=\text{O}$ can be thought to result from the larger bond length, reduced mass, and stretching frequency of the N-O group relative to those of the N-N group. (3) A requirement for phonon broadening of linewidths is that the final state, j , be significantly different from the initial state, i , such that vi-

brational excitation is possible. This criterion is met not only in XPS measurements of polar materials (i = ground state, j = one hole), but also in AES measurements as well (i = one hole, j = two holes).⁴ (We have, in fact, measured Auger-linewidth temperature effects in several insulating materials.) It is also clear why XPS linewidth measurements of any material involving core holes (e.g. $K\alpha_{1,2}$) do not reflect appreciable phonon broadening,⁷ since the i and j one-hole states are, as far as the lattice is concerned, virtually identical. This statement, however, is not true for valence-to-core x-ray transitions in which the i and j states are quite different.²

The authors are grateful to S. Doniach for several stimulating and significant discussions and to P. M. Platzman for helpful comments and suggestions.

¹For reviews on this topic, see M. H. L. Pryce, in *Phonons in Perfect Lattices and in Lattices with Point Imperfections*, edited by R. W. H. Stevenson (Oliver and Boyd, Edinburgh, Scotland, 1966), p. 403; J. J. Markham, *Rev. Mod. Phys.* **31**, 956 (1959).

²L. G. Parratt, *Rev. Mod. Phys.* **31**, 616 (1959).

³W. E. Spicer, *Phys. Rev.* **154**, 385 (1967).

⁴J. A. D. Matthew, *Surface Sci.* **20**, 183 (1970).

⁵R. M. Friedman, J. Hudis, and M. L. Perlman, *Phys. Rev. Lett.* **29**, 692 (1972); R. W. Shaw, Jr., and T. D. Thomas, *Phys. Rev. Lett.* **29**, 689 (1972).

⁶P. H. Citrin, *Phys. Rev. Lett.* **31**, 1164 (1973).

⁷P. H. Citrin, P. M. Eisenberger, W. C. Marra, T. Åberg, J. Utriainen, and E. Källne, *Phys. Rev. B* **10**, 1762 (1974).

⁸P. H. Citrin, in *Proceedings of the International Conference on Electron Spectroscopy*, Namur, Belgium, 16–19 April 1974 (to be published); P. H. Citrin, J. E. Rowe, and S. B. Christman, to be published.

⁹U. Geluis, S. Svensson, H. Siegbahn, E. Basilier, Å. Faxälv, and K. Siegbahn, reported at International Conference on Electron Spectroscopy, Namur, Belgium, 16–19 April 1974, and to be published.

¹⁰K. Huang and A. Rhys, *Proc. Roy. Soc., Ser. A* **208**, 352 (1951).

¹¹C. Kittel, *Quantum Theory of Solids* (Wiley, New York, 1963), pp. 137–142.

¹²A. W. Overhauser, footnote 108 in Ref. 2.

¹³P. H. Citrin and T. D. Thomas, *J. Chem. Phys.* **57**, 4446 (1972).

¹⁴S. P. Kowalczyk, F. R. McFeely, L. Ley, R. A. Pollak, and D. A. Shirley, *Phys. Rev. B* **8**, 3573 (1974).

¹⁵Coefficients of linear mixing expressing line shapes in the fitting routine have been calibrated against convoluted Lorentzian and Gaussian line shapes of known composition (G. K. Wertheim, M. A. Butler, K. W. West, and D. N. E. Buchanan, to be published). Previous interpretation of these coefficients (Ref. 6) had as-

sumed direct 1:1 correspondence between them and fractional compositions, leading to sizable overestimates of Lorentzian parentage.

¹⁶E. J. McGuire, Phys. Rev. A **3**, 1801 (1971).

¹⁷Wertheim, Butler, West, and Buchanan, Ref. 15.

¹⁸W. Meyer, J. Chem. Phys. **58**, 1017 (1973).

¹⁹U. Gelius, E. Basilier, S. Svensson, T. Bergmark,

and K. Siegbahn, J. Electron Spectrosc. Relat. Phenomena **2**, 405 (1974).

²⁰The S Franck-Condon overlap factors can be shown to obey a Poisson distribution (Ref. 1), the standard deviation of which is \sqrt{S} ; the full linewidth at half-maximum of such a distribution is proportional to $\hbar\omega_{LO}\sqrt{S} = (\Delta E\hbar\omega_{LO})^{1/2}$, the leading term in Eq. (1).

Probing the Superconducting Vortex Structure by Polarized- μ^+ Spin Precession

A. T. Fiory, D. E. Murnick, and M. Leventhal
Bell Laboratories, Murray Hill, New Jersey 07974

and

W. J. Kossler*
The College of William and Mary, Williamsburg, Virginia 23185
(Received 30 July 1974)

The magnetic field structure of vortices in the mixed state of a lead-indium alloy and of niobium was probed by stopped μ^+ particles. Fourier transforms of time-dependent spin-precession data contain a peak at the average internal field, which is also the applied field. For the alloy only there is a second peak at the saddle point of the internal field distribution. Motional averaging due to quantum diffusion of the muons at low temperatures can account for these results.

Recent experiments have demonstrated the usefulness of using polarized muons as microscopic probes of local magnetic fields in magnetic metals.¹ Positive muons can be considered as radioactive protons with known magnetic moment ($e\hbar/2m_\mu c$) and lifetime (2.2 μsec). The field on the muon is easily determined from the precession frequency of the anisotropic angular distribution of decay positrons ($\mu^+ \rightarrow e^+ + \nu_e + \bar{\nu}_\mu$). By analogy to H^+ , the μ^+ is presumed to reside at interstitial sites in metals.²

The muon spin-precession technique is analogous to the well-known time-dependent perturbed-angular-correlation method for common radioactive species. It was used to study the local magnetic field distribution in samples of $\text{Pb}_{0.90}\text{In}_{0.10}$ and Nb, type-II superconductors, in the mixed state. Our results indicate that the μ^+ particle remains highly mobile at low temperatures in Nb.

Previous experiments on the magnetic structure of the mixed state of type-II superconductors made use of such techniques as NMR,³ neutron diffraction,⁴ perturbed angular correlation,⁵ molecular beams,⁶ and decoration microscopy.⁷ From the results of such experiments, the prominent features of the mixed-state local field distribution expected in the muon-precession-frequency spectrum are a peak at the local field cor-

responding to the saddle-point location in the vortex lattice, B_s , and maximum and minimum cut-off fields.³ The periodic inhomogeneity created is expected to lead to both line broadening and a shift, since $B_s < B$, the average of the internal field. Experiments reported in this Letter were motivated by the attractiveness of applying a versatile new technique to a model example and the possibility of studying various dynamical effects.

Predictions of what the precession data should look like have been calculated before,⁸ but we have preferred a semiempirical approach. The precession angle as a function of time at a site \vec{r} in the vortex lattice can be derived from the expression

$$\theta(t) = \gamma_\mu t B \sum_{\vec{g}} F_{\vec{g}} \cos(\vec{g} \cdot \vec{r}),$$

where γ_μ is the gyromagnetic ratio of the muon and \vec{g} a reciprocal-vortex-lattice vector. Choosing zero time to correspond to zero phase is arbitrary. Values of the Fourier components $F_{\vec{g}}$ for our niobium specimen were interpolated from neutron-diffraction measurements on specimens of comparable purity.⁹ Similarly, measurements on an alloy of comparable Ginzburg-Landau parameter were used as a basis for calculating appropriate Fourier components for the lead-indium specimen.¹⁰